Available online at www.sciencedirect.com

SciVerse ScienceDirect

Ceramics International 39 (2013) 4757–4763

CERAMICS INTERNATIONAL

www.elsevier.com/locate/ceramint

Microwave- and conventional-hydrothermal synthesis of CuS, SnS and ZnS: Optical properties

Xinlong Yan[a,c], Elizebeth Michael[b], Sridhar Komarneni[c,*], Jeffrey R. Brownson[d], Zi-Feng Yan[a]

[a]State Key Laboratory of Heavy Oil Processing, CNPC Key Laboratory of Catalysis, China University of Petroleum, Qingdao 266555, PR China
[b]Department of Materials Science and Engineering, The Pennsylvania State University, University Park, PA 16802, USA
[c]Materials Research Institute, Materials Research Laboratory, The Pennsylvania State University, University Park, PA 16802, USA
[d]Department of Energy and Mineral Engineering, The Pennsylvania State University, University Park, PA 16802, USA

Received 21 September 2012; received in revised form 20 November 2012; accepted 21 November 2012
Available online 28 November 2012

Abstract

Sulfides of Cu, Sn and Zn were synthesized by conventional-hydrothermal (C-H) and microwave hydrothermal (M-H) methods using thioacetamide as a sulfide source. The synthesized CuS, SnS and ZnS were characterized by powder X-ray diffraction (XRD), scanning electron microscopy and UV–vis diffuse reflectance spectra. The results suggest that M-H process led to very rapid crystallization of all the sulfides compared to the C-H process. Band gaps of the CuS, SnS and ZnS were determined to be 1.8, 1.3 and 3.6, respectively matching the theoretical anticipated band gaps of 2.0, 1.2 and 3.54, respectively suggesting that pure phases were obtained. The three sulfides are potentially useful for the composite solid-state synthesis of kesterite, a photovoltaic material.

Keywords: Covellite; ZnS; SnS; Conventional-hydrothermal and Microwave-hydrothermal synthesis

1. Introduction

Copper sulfide, zinc sulfide, and tin (II) sulfide have come under increasing scrutiny over the past few years for their use in the synthesis of Kesterite, Cu_2ZnSnS_4 (CZTS). These binary chalcogenides have been used in both sputtering [1] and nanocomposite techniques [2] for the synthesis of this thin film photovoltaic absorber material. Copper sulfide is used in various semiconductor devices, such as solar cells, photodetectors, photothermal conversion devices, gas sensors, and microwave shielding coating [3]. Zinc sulfide is a wide band gap semiconductor; it has uses in optics as an infrared window material and is an alpha-ray detector, becoming luminescent when struck by alpha-rays [4]. Tin (II) sulfide has uses as a heterojunction material in photovoltaic devices, and in optoelectronic devices [5]. Sulfur volatility is a major obstacle to the stoichiometric processing of these binary chalcogenides, and, as a result, studies are being conducted into the optimal processing methods for these important materials.

Copper sulfide synthesis is typically accomplished via hydrothermal synthesis [6–8], although microwave irradiation and sonochemistry [9,10] have both been used as a means to form covellite copper (II) sulfide. Hydrothermal processing of copper nitrate and elemental sulfur in either dimethylformamide or ethylene glycol has been shown to produce copper sulfide nanoparticles [11]. Hydrothermal synthesis has also been successfully pursued using copper acetate and copper nitrate in thiourea and cetyltrimethylamonium bromide [12]. Typical hydrothermal processing times for covellite copper sulfide are 24 h if done by the traditional hydrothermal methods [12]. To make these methods more environmentally benign, processing temperatures and times must be decreased to reduce the energy cost. Other approaches, such as microwave irradiation,

*Corresponding author.
E-mail address: komarneni@psu.edu (S. Komarneni).

0272-8842/$ - see front matter © 2012 Elsevier Ltd and Techna Group S.r.l. All rights reserved.
http://dx.doi.org/10.1016/j.ceramint.2012.11.062

decompose copper chloride–thiourea complexes using microwaves irradiation to form covellite copper sulfide [9].

Zinc sulfide nanoparticle synthesis has been achieved through many solution-based syntheses [13]. For example, successful synthesis occurred through the reflux of zinc acetate dihydrate, 1-thioglycerol, and sodium sulfide nonahydrate in dimethylformamide and water; slightly basic conditions were maintained [14]. Another solution-based method involves the dehydration of solutions of zinc chloride in methanol and sulfur in 1-dodecanethiol followed by a reaction with oleylamine [15]. Although several greener methods have been developed [13], such as the hydrothermal processing of thiocarbamide, zinc acetate, and water at 140 °C for 5 h [16], the process may still be improved by the use of lower temperatures and processing times. Several other approaches have been explored, such as liquid–solid-solution processing [17], aging reaction mixtures [18], and chemical reduction [19]. Zinc sulfide spheres of about 150 nm were prepared by refluxing Zn nitrate, thioacetamide and polyvinylpyrrolidone (PVP) at 80 °C for 2 h [20] using a similar procedure reported previously [21].

Tin (II) sulfide formation has been accomplished using organic solvents for chemical syntheses. The organometallic complex $Sn[N[(SiCH_3)_3]_2]_2$ was used as a tin precursor and thioacetamide as a sulfur precursor in one such synthesis [22]. However, the organometallic complex is air sensitive, leading to strict processing conditions. Other chemical syntheses using organic solvents were attempted [23,24]. A more simple approach was used by Xu et. al in which $SnBr_2$ and Na_2S were combined in the presence of ethanolamines dissolved in ethylene glycol [25]. Thioglycolic acid-assisted hydrothermal processing of tin (II) sulfide was achieved using tin (II) chloride and sodium sulfide in an aqueous solution [26]. Tin (II) sulfide has also been formed successfully using chemical vapor deposition [27] and sputtering [28].

Because of our interest in kesterite as a photovoltaic material and in the composite processing technique for its preparation, we here report the synthesis of CuS, SnS and ZnS using thioacetamide as the sulfide source by the conventional-hydrothermal (C-H) method and compared it with the microwave-hydrothermal (M-H) method. Optical properties of the hydrothermally prepared sulfides are also reported. The CuS, SnS and ZnS prepared here are potentially useful as precursors to prepare kesterite by composite processing at high temperature in sulfur-rich environment.

2. Experimental section

2.1. Synthesis of CuS, ZnS and SnS

In a typical conventional-hydrothermal (C-H) synthesis, 5 mmol of zinc nitrate (Alfa Aesar), copper nitrate (Alfa Aesar, 98%–102%) or tin chloride (Sigma-Aldrich, 98%) were dissolved in 60 mL of distilled water. Then, 2 g of polyvinylpyrrolidone (PVP, M.W. 40000, Sigma-Aldrich) and 5 mmol of thioacetamide (Alfa Aesar, 98%) were added to each of the above solutions. After stirring at room temperature for 30 min, the mixtures were transferred into Teflon-lined stainless steel autoclave (Parr Reactor) and treated at three different temperatures (100 °C, 150 °C or 200 °C) for 4 h. Finally, the precipitates were separated from solutions by centrifugation and washed repeatedly with water and ethonal to remove all soluble salts.

The above mixtures were also subjected to microwave-hydrothermal (M-H) synthesis, which was performed using the MARS5 microwave digestion system [29]. This system controls the temperature and/or pressure. The temperature can be measured using an optical probe encased in a sapphire tube. The synthesis was performed under static conditions at 100° or 150 °C for 15 to 45 min using 300 W of microwave power. The solid products were collected as described above for the C-H method.

2.2. Characterization

X-ray diffraction (XRD) patterns for the samples were recorded on a Panalytical Xpert PRO X-ray diffractometer with Cu Kα radiation ($\lambda = 1.5406$ Å, 45 KV, 40 mA). Scanning electron microscopy (SEM) was performed using a Hitachi S-4800 field emission scanning electron microscope (accelerating voltage: 3.0 kV).

UV–vis characterization of CuS, SnS and ZnS was done using a Perkin-Elmer Lambda 950 UV/VIS/NIR Spectrophotometer. A 150 mm integrating sphere attachment in diffuse reflectance mode was used for collection of UV–vis spectra. Although this instrument is accurate over a 250 nm to 2500 nm range, here we used a scan range of 600 nm to 1200 nm for collecting UV–vis spectra. The scan range was expanded midway through data collection to encompass a range of 500 nm to 1500 nm using a step size of 2 nm. A photomultiplier tube was used as the detector in the ultraviolet and visible regions of the scan range while PbS was used in the near infrared region.

3. Results and discussion

Results of various crystallized CuS, ZnS and SnS samples prepared by C-H conditions at different temperatures for 4 h are presented in Table 1. Table 2 presents the results of the three sulfides crystallized at different temperatures and durations under M-H conditions. The mechanism of formation of sulfides can be represented as follows:

$$M^{2+} + CH_3C(S)NH_2 + H_2O \rightarrow MS + CH_3C(O)NH_2 + 2\,H^+$$
(M = Cu, Zn and Sn)

The main purpose of thioacetamide is to supply sulfide under slow release by the hydrolysis/decomposition of the thioacetamide and nucleation for the formation of sulfides. During the above reaction, the reaction product $CH_3C(O)NH_2$ as well as excess thioacetamide are expected to stay in solution and not incorporated in the solids. All the organics have been removed by through washing of the solids after the

Table 1
CuS, ZnS and SnS samples prepared by the conventional hydrothermal conditions at different temperatures.

Sample	Chemicals[a]	Crystallization temperature (°C)	Crystallizationtime (h)	XRD
CuS	$Cu(NO_3)_2$, PVP	100	4	CuS formed
CuS[b]	$Cu(NO_3)_2$, PVP	150	4	CuS formed
CuS	$Cu(NO_3)_2$, PVP	200	4	CuS formed
ZnS	$Zn(NO_3)_2$, PVP	100	4	ZnS formed
ZnS[b]	$Zn(NO_3)_2$, PVP	150	4	ZnS formed
ZnS	$Zn(NO_3)_2$, PVP	200	4	ZnS formed
SnS	$SnCl_2$, PVP	100	4	SnS formed
SnS[b]	$SnCl_2$, PVP	150	4	SnS formed
SnS	$SnCl_2$, PVP	200	4	SnS formed

[a]The sulfide to metal ratio is 1:1 for all the samples and thioacetamide is the sulfide source in all syntheses.
[b]These samples were also prepared without PVP.

Table 2
CuS, ZnS and SnS samples prepared by the microwave hydrothermal method at different temperatures and durations of treatment.

Sample	Chemicals[a]	Crystallization		XRD
		Temperature (°C)	Duration (min)	
CuS	$Cu(NO_3)_2$, PVP	150	15	CuS formed
CuS	$Cu(NO_3)_2$, PVP	150	30	CuS formed
CuS	$Cu(NO_3)_2$, PVP	150	45	CuS formed
CuS	$Cu(NO_3)_2$, PVP	175	15	CuS formed
ZnS	$Zn(NO_3)_2$, PVP	150	15	ZnS formed
ZnS	$Zn(NO_3)_2$, PVP	150	30	ZnS formed
ZnS	$Zn(NO_3)_2$, PVP	150	45	ZnS formed
ZnS	$Zn(NO_3)_2$, PVP	175	15	ZnS formed
SnS	$SnCl_2$, PVP	150	15	SnS formed
SnS	$SnCl_2$, PVP	150	30	SnS formed
SnS	$SnCl_2$, PVP	150	45	SnS formed
SnS	$SnCl_2$, PVP	175	15	SnS formed

[a]Thioacetamide is the sulfide source in all syntheses.

reaction. Well-crystallized sulfides were obtained as indicated by sharp peaks in their XRD patterns (Figs. 1 and 2) in all cases. Typical powder XRD patterns of CuS and ZnS prepared by the C-H method at 150 °C/4 h and M-H method at 150 °C/15 min are shown in Fig. 1. The diffraction peaks of both the CuS samples by the C-H and M-H methods could be indexed to the standard diffraction data of the corresponding hexagonal covellite, CuS (JCPDS no:060464). Similarly, the diffraction peaks of both the ZnS samples by the C-H and M-H methods could be indexed to the standard diffraction data of the corresponding hexagonal ZnS (JCPDS no:83-2124). No other characteristic peaks were observed, indicating that the synthesized products were pure. The sharp peaks revealed that the obtained samples were of good crystallinity.

Fig. 2 shows the typical XRD patterns of the SnS product prepared by the C-H method at different temperatures for 4 h and the M-H method at 150 °C for 15 min. It can be seen that all the diffraction peaks could be indexed to the standard diffraction data of the corresponding herzenbergite, SnS

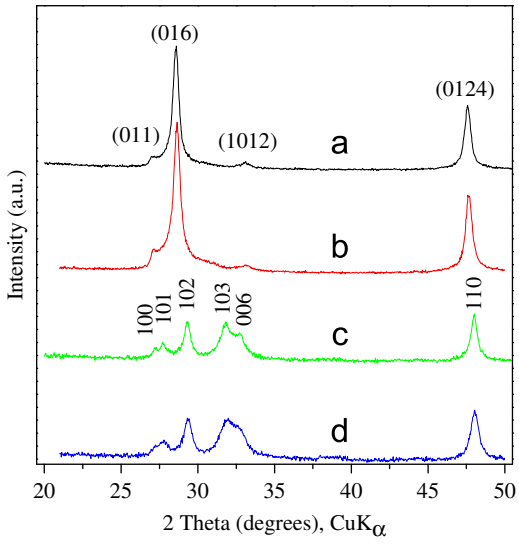

Fig. 1. XRD patterns of ZnS and CuS prepared at 150 °C: (a) ZnS by the C-H method for 4 h, (b) ZnS by the M-H method for 15 min, (c) CuS by the C-H method for 4 h and (d) CuS by the M-H method for 15 min.

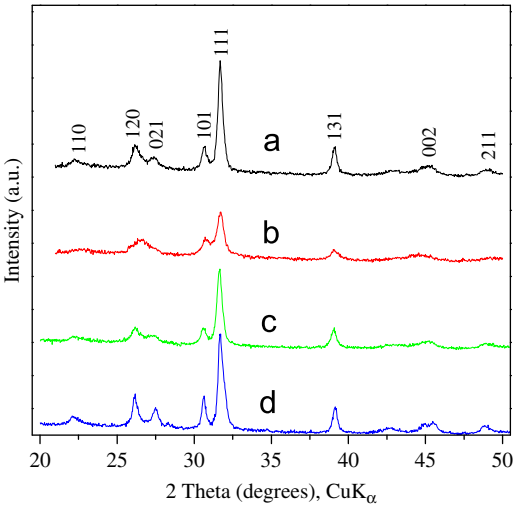

Fig. 2. XRD patterns of SnS prepared at different temperatures by the M-H and C-H methods: (a) M-H method at 150 °C for 15 min, (b) C-H method at 100 °C for 4 h, (c) C-H method at 150 °C for 4 h and (d) C-H method at 200 °C for 4 h.

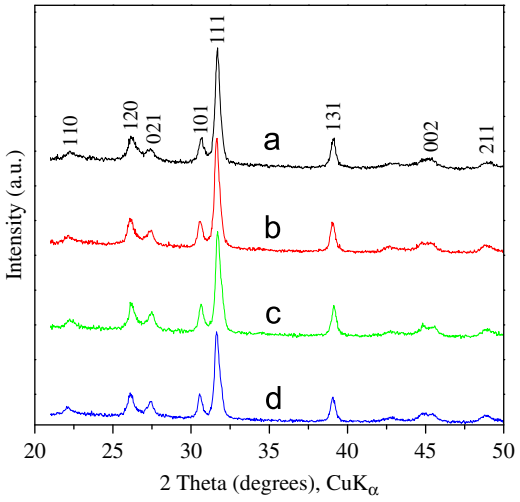

Fig. 3. XRD patterns of SnS prepared by the microwave hydrothermal method at different temperatures and durations: (a) SnS at 150 °C for 15 min, (b) SnS at 150 °C for 30 min, (c) SnS at 150 °C for 45 min and (d) SnS at 175 °C for 15 min.

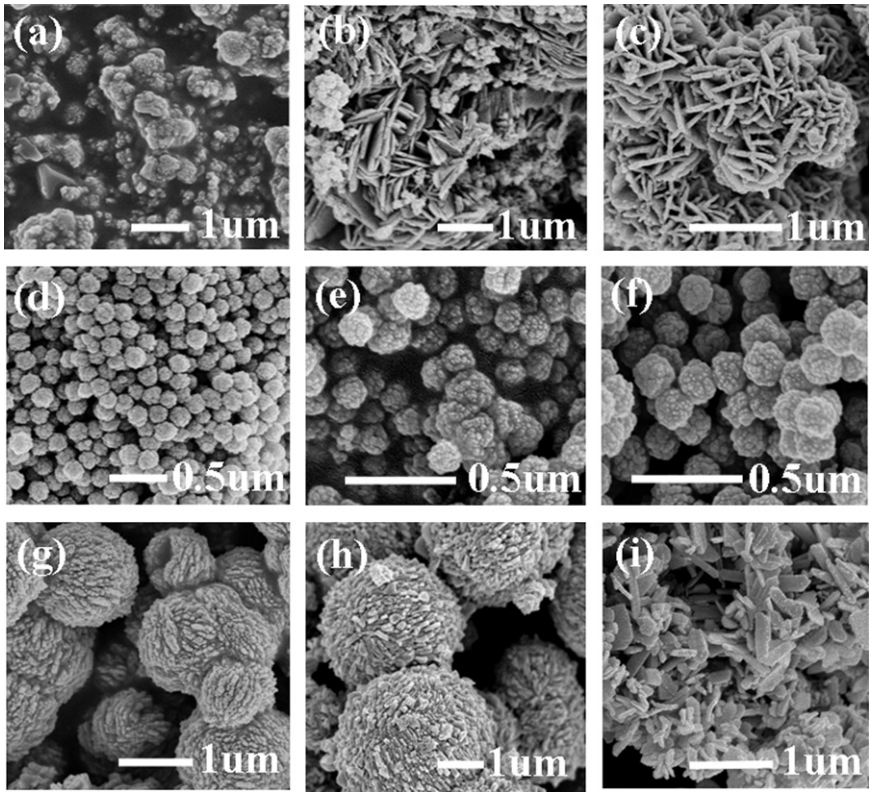

Fig. 4. SEM images of sulfides prepared by the conventional hydrothermal method for 4 h: (a) CuS at 100 °C, (b) CuS at 150 °C, (c) CuS at 200 °C, (d) ZnS at 100 °C, (e) ZnS at 150 °C, (f) ZnS at 200 °C, (g) SnS at 100 °C, (h) SnS at 150 °C and (i) SnS at 200 °C.

(JCPDS no:33-1375). No other characteristic peaks were observed, indicating that the synthetic products were pure. When the hydrothermal temperature was increased from 100 °C to 200 °C under C-H conditions, the intensity of the peaks increased (Fig. 2b–d), indicating that the crystallinity of SnS improved as a function of temperature, as expected because of Ostwald ripening. Using the M-H method at 150 °C, only 15 min were needed to achieve high intensity of CuS and ZnS peaks while the samples prepared by the C-H method at the same temperature needed 4 h (Fig. 1). The SnS peaks at 150 °C by the M-H method prepared in 15 min (Fig. 2a) were as strong as those by the sample prepared by C-H method at 200 °C for 4 h (Fig. 2d). Compared with the C-H method, M-H treatment has led to faster crystallization

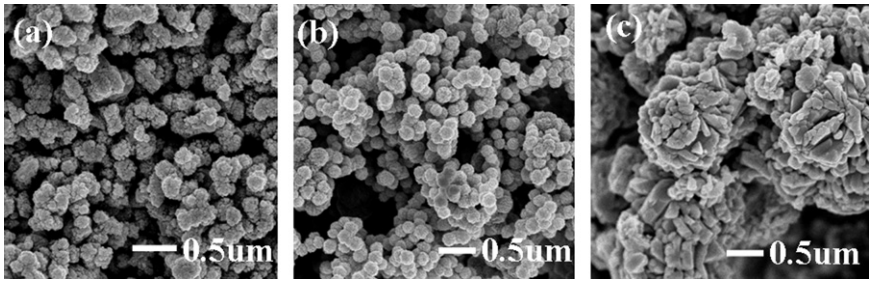

Fig. 5. SEM images of sulfides prepared by the microwave hydrothermal method for 15 min: (a) CuS at 150 °C, (b) ZnS at 150 °C and (c) SnS at 150 °C.

of all three sulfides investigated here confirming many previous results which reported faster kinetics of synthesis or crystallization of many materials under M-H conditions [30–33]. The mechanism of faster crystallization by the M-H method can be explained by the localized superheating [34] where nucleation began rapidly and therefore, led to faster crystallization by growth.

Fig. 3 shows the XRD patterns of SnS prepared by the microwave hydrothermal method at different temperatures and durations. It appears that the crystallinity of the SnS did not change either with time or temperature of treatment under the M-H conditions used here. This result suggests that SnS is very easy to crystallize and once crystallized there is little growth of the crystals by Ostwald ripening probably because of the low solubility of SnS.

The role of synthesis temperature on particle size and morphology of the various sulfides prepared at different temperatures was investigated and the results are shown in Fig. 4. Spherical aggregates of particles of CuS formed at 100 °C (Fig. 4a) while spherical aggregates of particles as well as blades (Fig. 4b) formed at 150 °C, apparently some of the particles changed to blades at the latter temperature. At 200 °C, spherical aggregates of blades only resulted (Fig. 4c). Thus the morphology of CuS changed as a function of temperature. In the case of ZnS, microspheres of aggregated nanoparticles were observed at all temperatures with little or no change in morphology or size (Fig. 4d–f) while SnS yielded aggregates of brick-like particles at 100 °C and 150 °C (Fig. 4g and h) which grew to larger size and became separated at 200 °C (Fig. 4i).

The role of microwaves on the morphology and particle size of CuS, ZnS and SnS was investigated and the results are shown in Fig. 5, which shows the SEM images of CuS, ZnS and SnS at 150 °C prepared by the M-H method. The morphology of CuS under C-H conditions at 150 °C is spherical aggregates of particles as well as blades (Fig. 6a) while the morphology under M-H conditions is aggregated nanoparticles at the same temperature (Fig. 6b). It appears that the aggregated spherical particles started to transform to blades because of longer treatment time during the C-H conditions compared to the M-H conditions where the treatment time was only 15 min. Blades of spheres is the morphology of SnS at 200 °C (Fig. 5c) and this morphology perhaps could also be obtained with longer treatment time based on the above results at 150 °C under C-H conditions

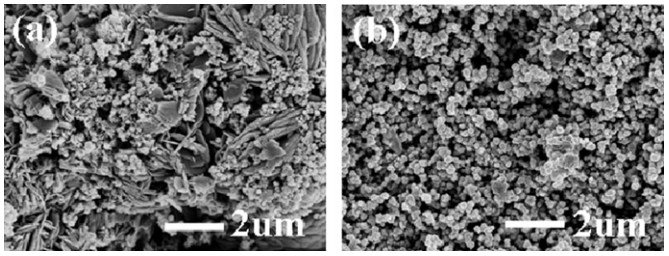

Fig. 6. SEM images of CuS samples prepared at 150 °C by the conventional hydrothermal method for 4 h (a) and the microwave hydrothermal method for 15 min (b).

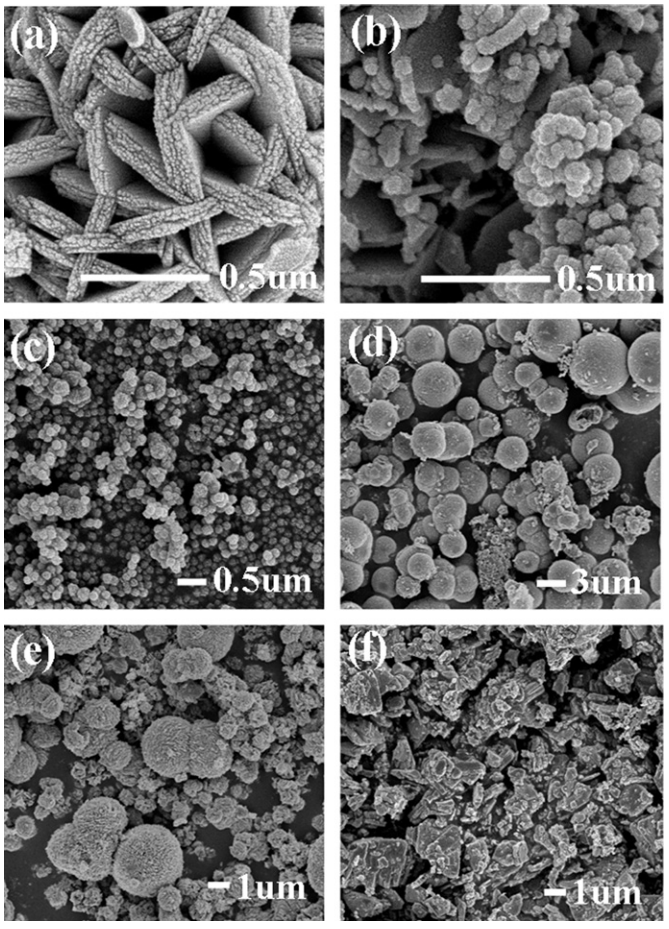

Fig. 7. SEM images of CuS, ZnS and SnS samples prepared with and without PVP at 150 °C for 4 h by the conventional hydrothermal method: (a) CuS with PVP, (b) CuS without PVP, (c) ZnS with PVP, (d) ZnS without PVP, (e) SnS with PVP and (f) SnS without PVP.

which showed partial conversion to blades after treatment for 4 h (Fig. 6a). The morphology and particle size of ZnS at 150 °C under M-H (Fig. 5b) and C-H (Fig. 4e) are the same. Similarly, the morphology and particle size of SnS at 150 °C under M-H (Fig. 5c) and C-H (Fig. 4h) did not change much except that slightly larger crystals formed and aggregated in the former. Syntheses by M-H and C-H yielded aggregated particles of various sulfides under the present conditions.

Fig. 7 shows the SEM pictures of CuS, ZnS and SnS samples prepared with and without PVP at 150 °C for 4 h by the conventional hydrothermal method. In the case of CuS synthesis with PVP, mainly aggregated blades formed while in the absence of PVP different morphologies were obtained and some very large crystals formed (Fig. 7a and b). A clear role of PVP can be seen with the synthesis of ZnS as much smaller Zns particles were obtained with PVP while very large spheres were obtained without PVP. The reduction in particle size is expected with PVP as the PVP molecules block the crystals from growing as has been documented before [29]. In the case of SnS, a wide particle size range of spheres (Fig. 7e) was obtained in the presence of PVP while in the absence of PVP, large block-like particles (Fig. 7f) were obtained. Thus the behavior of PVP is different with different sulfides in controlling the morphology. Further studies are needed to clearly delineate the role of PVP with each sulfide but these studies are beyond the scope of current study.

Fig. 8 shows the UV–vis diffuse reflectance spectra of the three sulfides while Fig. 9 shows the band gaps calculated from Kubelka–Munk transformations of all the samples. The determined band gaps of CuS, SnS and ZnS are 1.8, 1.3 and 3.6, respectively compared to the anticipated bandgaps of 2.0, 1.2 and 3.54, respectively. The small differences in band gap values between the experimentally determined values and the theoretical values could be explained by the particle sizes as has been shown previously for ZnO [35]. A detailed explanation of these small differences in band gaps is, however, beyond the scope of this research. The main reason why we measured the band gap values is to show a close match of the determined and expected band gap values which may suggest that the synthesized materials

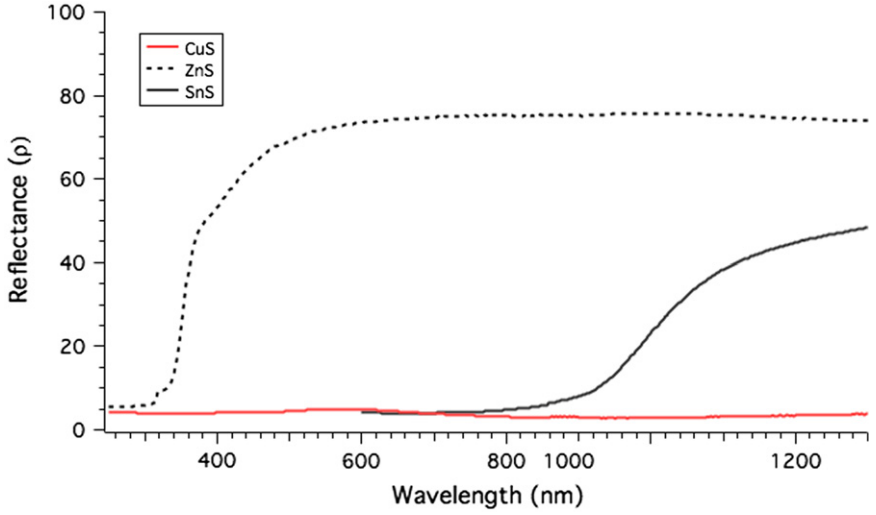

Fig. 8. UV–vis spectra of CuS, ZnS and SnS.

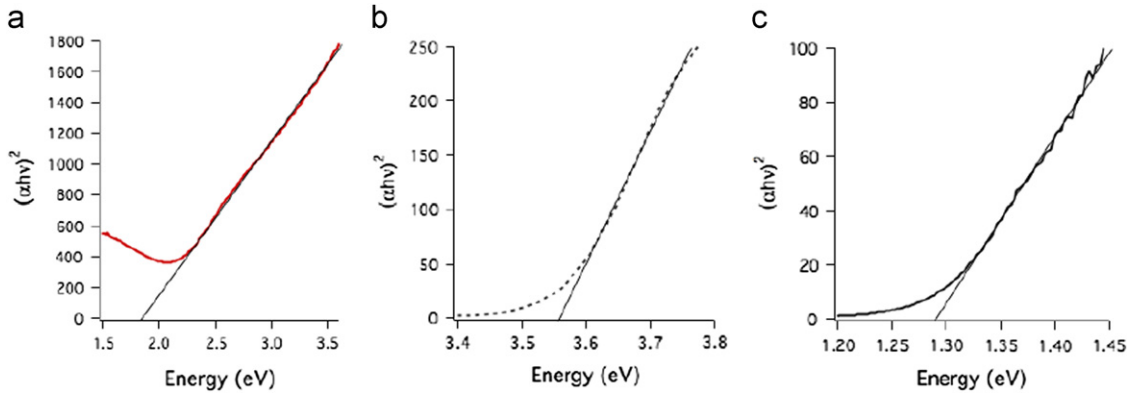

Fig. 9. Band gaps of CuS, ZnS and SnS from Kubelka–Munk transformation. (a) CuS (Dir 1.8 eV); (b) ZnS (Dir 3.6 eV) and (c) SnS (Dir 1.3eV).

are pure phases as has already been shown above by XRD.

4. Conclusions

Both conventional- and microwave-hydrothermal methods are highly suitable for green processing of CuS, SnS and ZnS. All the sulfides could be synthesized in as little time as 15 min in the temperature range of 100–200 °C using the microwave-assisted reactions.

Acknowledgment

Xinlong Yan thanks the China Scholarship Council (CSC) for the financial support.

References

[1] K. Ito, T. Nakazawa, Electrical and optical properties of stannite-type quaternary semiconductor thin films, Japanese Journal of Applied Physics 27 (1988) 2094–2097.
[2] Y. Wang, H. Gong, Low temperature synthesized quaternary chalcogenide cu_2znsns_4 from nano-crystallite binary sulfides, Journal of the Electrochemical Society 158 (2011) 800–803.
[3] V. Krylova, M. Andrulevičius, Optical, XPS and XRD studies of semiconducting copper sulfide layers on a polyamide film, International Journal of Photoenergy 2009 (2009) Article ID 304308.
[4] S.K. Lee, S.Y. Kang, D.Y. Jang, C.H. Lee, S.M. Kang, B.H. Kang, W.G. Lee, Y.K. Kim, Comparison of new simple methods in fabricating ZnS(Ag) scintillators for detecting alpha particles, Progress in Nuclear Science and Technology 1 (2011) 194–197.
[5] S.G. Hickey, C. Waurisch, B. Rellinghaus, A. Eychmuller, Size and shape control of colloidally synthesized IV – VI nanoparticulate tin (II) sulfide, Journal of the American Chemical Society 130 (2008) 14978–14980.
[6] C. Tan, R. Lu, P. Xue, C. Bao, Y. Zhao, Synthesis of CuS nanoribbons templated by hydrogel, Materials Chemistry and Physics 112 (2008) 500–503.
[7] Y.C. Zhang, T. Qiao, X.Y. Hu, A simple hydrothermal route to nanocrystalline CuS, Journal of Crystal Growth 268 (2004) 64–70.
[8] K. Tang, D. Chen, Y. Liu, G. Shen, H. Zheng, Y. Qian, Shape-controlled synthesis of copper sulfide nanocrystals via a soft solution route, Journal of Crystal Growth 263 (2004) 232–236.
[9] A. Tadjarodi, D. Khaledi, Preparation of CuS Nanoparticles by Microwave Irradiation, in: Proceedings of the 14th International Electronic Conference on Synthetic Organic Chemistry, 2010.
[10] H. Wang, J.R. Zhang, X.N. Shao, S. Xu, J.J. Zhu, Preparation of copper monosulfide and nickel monosulfide nanoparticles by sonochemical method, Materials Letters 55 (2002) 253–258.
[11] Fei Li, T. Kong, W. Bi, D. Li, Z. Li, X. Huang, Synthesis and optical properties of CuS nanoplate-based architectures by a solvothermal method, Applied Surface Science 255 (2009) 6285–6289.
[12] K. Zare, M. Darouie, F. Mollaamin, M. Monajjemi, An investigation on a mild hydrothermal route to CuS nano and submicro structures, International Journal of Physical Sciences 6 (2011) 2536–2540.
[13] X. Fang, T. Zhai, U.K. Gautam, L. Li, L. Wu, Y. Bando, D. Golberg, ZnS nanostructures: from synthesis to applications, Progress in Materials Science 56 (2011) 175–287.
[14] J. Nanda, S. Sapra, D.D. SarmaNanda, Size-selected zinc sulfide nanocrystallites: synthesis, structure, and optical studies, Chemistry of Materials 12 (2000) 1018–1024.
[15] T. Kuzuya, Y. Tai, S. Yamamuro, K. Sumiyama, Synthesis of copper and zinc sulfide nanocrystals via thermolysis of the polymetallic thiolate cage, Science and Technology of Advanced Materials 6 (2005) 84–90.
[16] H.J. Liu, Y.H. Ni, M. Han, Q. Liu, Z. Xu, J.M. Hong, X. Ma, A facile template-free route for the synthesis of hollow hexagonal ZnS nano-and submicro-spheres, Nanotechnology 16 (2005) 2908–2912.
[17] X. Wang, J. Zhuang, Q. Peng, Y.D. Li, A general strategy for nanocrystal synthesis, Nature 437 (2005) 121–124.
[18] J.H. Yu, J. Joo, H.M. Park, S. Baik, Y.W. Kim, S.C. Kim, T. hyeon, Synthesis of quantum-sized cubic ZnS nanorods by the oriented attachment mechanism, Journal of the American Chemical Society 127 (2005) 5662–5670.
[19] W. Wang, I. Germanenko, M.S. EI-Shall, Room-temperature synthesis and characterization of nanocrystalline CdS, ZnS and $Cd_xZn_{1-x}S$, Chemistry of Materials 14 (2002) 3028–3033.
[20] S.K. Panda, A. Datta, S. Chaudhuri, Nearly monodispersed ZnS nanospheres: synthesis and optical properties, Chemical Physics Letters 440 (2007) 235–238.
[21] Y.D. Kim, K. Sonezaki, H. Maeda, A. Kato, Sintering behaviour of monodispersed ZnS powders, Journal of Materials Science 32 (1997) 5101–5106.
[22] S.G. Hickey, C. Waurisch, B. Rellinghaus, A. Eychmüller, Size and shape control of colloidally synthesized IV – VI nanoparticulate tin(II) sulfide, Journal of the American Chemical Society 130 (2008) 14978–14980.
[23] H. Liu, Y. Liu, Z. Wang, P. He, Facile synthesis of monodisperse, size-tunable SnS nanoparticles potentially for solar cell energy conversion, Nanotechnology 21 (2010) 105707.
[24] J. Ning, K. Men, G. Xiao, L. Wang, Q. Dai, B. Zou, B. Liu, G. Zou, Facile synthesis of IV–VI SnS nanocrystals with shape and size control: nanoparticles, nanoflowers and amorphous nanosheets, Nanoscale 2 (2010) 1699–1703.
[25] Y. Xu, A.S. Najeh, R.D. Tilley, Synthesis and size dependent reflectance study of water soluble sns nanoparticles, Nanomaterials 2 (2012) 54–64.
[26] H. Zhu, D. Yang, Y. Ji, H. Zhang, X. Shen, Two-dimensional SnS nanosheets fabricated by a novel hydrothermal method, Journal of Materials Science 40 (2005) 591–595.
[27] A.T. Kana, T.G. Hibbert, M.F. Mahon, K.C. Molloy, I.P. Parkin, L.S. Price, Organotin unsymmetric dithiocarbamates: synthesis, formation and characterization of tin (II) sulfide films by atmospheric pressure chemical vapor deposition, Polyhedron 20 (2001) 2989–2995.
[28] K. Hartman, J.L. Johnson, M.I. Bertoni, D. Recht, M.J. Aziz, M.A. Scarpulla, T. Buonassisi, SnS thin-films by RF sputtering at room temperature, Thin Solid Films 519 (2011) 7421–7424.
[29] S. Komarneni, D. Li, B. Newalkar, H. Katsuki, A.S. Bhalla, Microwave-polyol process for Pt and Ag nanoparticles, Langmuir 18 (2002) 5959–5962.
[30] S. Komarneni, R. Roy, Titania gel spheres by a new sol-gel process, Materials Letters 3 (1985) 165–167.
[31] S. Komarneni, R. Roy, Q.H. Li, Microwave-hydrothermal synthesis of ceramic powders, Materials Research Bulletin 27 (1992) 1393–1405.
[32] S. Komarneni, Q. Li, K.M. Stefansson, R. Roy, Microwave-hydrothermal processing for synthesis of electroceramic powders, Journal of Materials Research 8 (1993) 3176–3183.
[33] S. Komarneni, Q.H. Li, R. Roy, Microwave-hydrothermal processing for synthesis of layered and network phosphates, Journal of Materials Chemistry 4 (1994) 1903–1906.
[34] B.L. Hayes, in: Microwave Synthesis — Chemistry at the Speed of Light, CEM Publishing, Matthews NC, 2002, p. 295.
[35] K.-F. Lin, H.-M. Cheng, H.-C. Hsu, L.-J. Lin, W.-F. Hsieh, Band gap variation of size-controlled ZnO quantum dots synthesized by sol–gel method, Chemical Physics Letters 409 (2005) 208–211.